Mathematics

AIMS Mathematics, 11(5): 12621–12649.
DOI: 10.3934/math.2026519
Received: 02 March 2026
Revised: 07 April 2026
Accepted: 10 April 2026
Published: 08 May 2026

https://www.aimspress.com/journal/Math

Research article

Exact and entropy-based nonparametric tests for exponentiality against increasing failure rate alternatives

Anfal A. Alqefari*

Department of Statistics and Operations Research, College of Science, Qassim University, P.O. Box 6644, Buraydah 51482, Saudi Arabia

* **Correspondence:** aa.alqefari@qu.edu.sa; Tel.: +966-541461447.

Abstract: Testing exponentiality against increasing failure rate (IFR) alternatives is a central problem in reliability theory with direct implications for aging characterization and maintenance optimization. In this paper, I introduce a novel entropy-based nonparametric test family constructed from fractional generalized cumulative residual entropy (FGCRE). The proposed statistics were formulated as scale-invariant L-functionals indexed by a tuning parameter, enabling adaptive sensitivity to diverse forms and magnitudes of IFR departures. A principal contribution of this work is the derivation of the exact finite-sample null distribution under exponentiality through a normalized spacing representation, thereby permitting fully exact, distribution-free inference without reliance on asymptotic approximations. Extensive Monte Carlo simulations demonstrated that the proposed test exhibits consistently strong and stable power, exceeding 0.85 in moderate sample sizes under Weibull alternatives and outperforming several established procedures, particularly in challenging discrimination regimes. Applications to real datasets from reliability engineering and environmental studies further confirmed the practical effectiveness of the proposed methodology in detecting positive aging behavior. Overall, the proposed framework offers a theoretically rigorous, flexible, and computationally efficient tool for exact and asymptotic testing of exponentiality against IFR alternatives.

Keywords: fractional generalized cumulative residual entropy; exponentiality testing; increasing failure rate; exact null distribution; L-statistics; reliability analysis; scale invariance
Mathematics Subject Classification: 60E15, 62G10, 62N05, 94A17

1. Introduction

The exponential distribution plays a foundational role in reliability theory, survival analysis, and applied probability. Its prominence stems not only from analytical tractability but also from its structural characterization through the memoryless property: Under exponentiality, the remaining lifetime of a functioning unit is stochastically independent of its age. In reliability contexts, this corresponds to systems whose failures are driven by random external shocks occurring according to a homogeneous Poisson process. Such models are appropriate for components that do not experience progressive deterioration, including certain electronic devices and shock-sensitive elements. Despite its convenience, the exponential assumption is frequently violated in practice. Many engineering systems, biological organisms, and structural components are subject to cumulative degradation, leading to increasing risk over time. This phenomenon is captured by the class of increasing failure rate (IFR) distributions, which formalize positive aging behavior and constitute one of the most fundamental aging classes in reliability theory.

Let X be a nonnegative random variable with cumulative distribution function F and survival function $\bar{F}(x) = 1 - F(x)$. The distribution of X is said to be IFR if its hazard rate function

$$\lambda(x) = \frac{f(x)}{\bar{F}(x)} \text{ is increasing in } x > 0.$$

Equivalently, the conditional survival function

$$\bar{F}(x;t) = \frac{\bar{F}(x+t)}{\bar{F}(t)} \text{ is decreasing in } t > 0 \text{ for each fixed } x \geq 0.$$

Classical examples of IFR models include the gamma, linear failure rate, Makeham, Pareto, and Weibull families, all of which arise naturally in reliability and life-testing applications. Testing the null hypothesis of exponentiality against increasing failure rate (IFR) alternatives is therefore a central and long-standing problem in statistical reliability analysis. From an operational standpoint, rejecting exponentiality in favor of IFR has immediate implications, as it signals the presence of progressive aging and thus supports preventive maintenance, replacement strategies, and warranty adjustments. Consequently, the development of powerful and theoretically sound nonparametric procedures for this problem has attracted sustained attention over several decades.

Early contributions include the spacing-based rank test of Proschan and Pyke [1], followed by asymptotic power investigations by Bickel and Doksum [2] and related foundational work by Bickel [3] and Barlow and Proschan [4]. Barlow and Doksum [5] established minimax optimality results for total time on test (TTT)-based procedures, linking convex orderings to IFR detection. Subsequent developments introduced U-statistic approaches (Ahmad [6]; Deshpande and Kochar [7]), scaled TTT-transform tests (Klefsjö [8]), graphical and functional methods (Aly [9]), and L-statistic constructions (Mitra and Anis [10]). Anis [11] further developed parametric families of tests and derived exact and asymptotic properties, thereby enriching the methodological landscape of exponentiality testing.

In addition to this classical literature, there has been witnessed increasing interest in entropy-based and information-theoretic measures for reliability analysis, aging characterization, and uncertainty quantification. In particular, fractional generalized cumulative residual entropy (FGCRE) and its extensions have emerged as powerful tools due to their strong connections with stochastic

orders, aging properties, and structural characteristics of lifetime distributions; see, for example, Di Crescenzo et al. [12], Alqefari et al. [13], Alomani and Kayid [14], Asadi et al. [15], and Kayid and Shrahili [16]. These developments highlight the growing role of entropy-based measures as flexible and conceptually unified tools for modeling and inference in reliability contexts.

Despite this progress, most entropy-based contributions have focused mostly on distributional characterization and asymptotic inference, and have not led to exact and practically implementable hypothesis testing procedures for exponentiality against IFR alternatives. By contrast, classical nonparametric tests provide well-established solutions, but are typically constructed as single-statistic procedures with fixed sensitivity structures and limited adaptability.

Motivated by this gap, in this paper I develop an exact entropy-based nonparametric test family for exponentiality against IFR alternatives. The proposed method is constructed from a deviation functional derived from FGCRE and leads to a class of scale-invariant L-statistics indexed by a tuning parameter, enabling adaptive sensitivity to different magnitudes and patterns of departure from exponentiality. Most importantly, by exploiting a normalized spacing representation under the exponential model, I derive an exact finite-sample null distribution for the proposed statistic, thereby enabling fully exact inference within the exponential family. To the best of my knowledge, such a combination of entropy-based construction, scale invariance, and exact finite-sample distributional theory has not been established in the literature on entropy-based tests for exponentiality against IFR alternatives. This exact distributional result is complemented by an asymptotic normality theory, providing a unified inferential framework applicable in small- and large-sample settings. Extensive Monte Carlo simulations demonstrate that the proposed entropy-based family achieves strong and stable power performance across IFR alternatives, including linear failure rate, Makeham, and Weibull models, and frequently outperforms established competitors. Applications to real reliability and environmental datasets further illustrate the practical effectiveness of the proposed methodology in detecting positive aging behavior. The proposed procedure is tailored for detecting positive aging in the IFR direction, and its applicability to other types of departures from exponentiality is beyond the scope of this work.

The remainder of the paper is organized as follows. In Section 2 the entropy-based deviation functional and constructs the test statistic family. In Section 3 the exact finite-sample null distribution and derive asymptotic results. In Section 4 simulation studies and real-data analyses. In Section 5 a discussion of theoretical implications and directions for future research.

2. Measure of deviation from exponentiality

In this section, I develop a deviation functional that quantifies the departure of an IFR distribution from the exponential family. Let

$$\mathcal{C} = \left\{F(x) = 1 - e^{-\theta x}; x \geq 0, \theta > 0\right\}$$

denote the class of exponential distributions. My objective is to test

$$H_0: F \in \mathcal{C} \text{ versus } H_1: F \in \text{IFR} \setminus \mathcal{C}$$

based on an independent and identically distributed sample $X_1, X_2, \ldots, X_n$ drawn from a distribution with cumulative distribution function F and density f.

2.1. Deviation functional based on Hazard monotonicity

If X follows an IFR distribution, its hazard rate $\lambda(x)$ is non-decreasing, implying that $\lambda(s) \leq \lambda(t)$ for all $0 < s \leq t$. To quantify the departure from hazard-rate constancy, define

$$\delta(t) = \int_0^t [\lambda(t) - \lambda(s)]ds = t\lambda(t) - \Lambda(t), t > 0, \tag{1}$$

where

$$\Lambda(t) = \int_0^t \lambda(s)ds = -\log \bar{F}(t)$$

is the cumulative hazard function. Under the IFR assumption, $\delta(t) \geq 0$ for all $t > 0$, and $\delta(t) = 0$ if and only if $\lambda(\cdot)$ is constant, i.e., $F \in \mathcal{C}$. Thus, $\delta(t)$ provides a pointwise measure of deviation from exponentiality.

2.2. Entropy-weighted global measure

To aggregate this local deviation over the support, introduce the weight function

$$w_\beta(t) = \frac{\bar{F}(t)\Lambda^{\beta-1}(t)}{\Gamma(\beta+1)}, \qquad \beta > 0,$$

where $\Gamma(\cdot)$ is the gamma function. Multiplying $\delta(t)$ by $w_\beta(t)$ and integrating over $(0, \infty)$

$$\begin{aligned}\mathbb{T}_\beta(F) &= \int_0^\infty w_\beta(t)\delta(t)dt \\ &= \frac{1}{\Gamma(\beta+1)}\int_0^\infty \bar{F}(t)\Lambda^{\beta-1}(t)[t\lambda(t) - \Lambda(t)]dt \\ &= \frac{1}{\Gamma(\beta+1)}\int_0^\infty tf(t)\Lambda^{\beta-1}(t)dt - \frac{1}{\Gamma(\beta+1)}\int_0^\infty \bar{F}(t)\Lambda^{\beta}(t)dt \\ &= \tfrac{1}{\Gamma(\beta+1)}\mathbb{E}\left[X\Lambda^{\beta-1}(X)\right] - \mathcal{E}_\beta(X). \end{aligned} \tag{2}$$

Using $f(t) = \lambda(t)\bar{F}(t)$, I obtain

$$\mathbb{T}_\beta(F) = \frac{1}{\Gamma(\beta+1)}\mathbb{E}\left[X\Lambda^{\beta-1}(X)\right] - \mathcal{E}_\beta(X),$$

where

$$\mathcal{E}_\beta(X) = \frac{1}{\Gamma(\beta+1)}\int_0^\infty \bar{F}(t)\Lambda^{\beta}(t)dt, \qquad \beta > 0,$$

is the FGCRE introduced in Di Crescenzo et al. [12].

2.3. 2.3 Connection with fractional entropy and Bayes risk

The FGCRE possesses a natural decision-theoretic interpretation; see Kayid and Shrahili [16]. Let $X_t = [X - t \mid X > t]$. denote the residual lifetime beyond t, and define the mean residual life function

$$\mu(t) = \mathbb{E}_{X>t}[X - t \mid X > t], t \geq 0.$$

Under quadratic loss, $\mu(t)$ minimizes the conditional risk. As demonstrated by Asadi et al. [15], integrating this local risk with respect to an appropriate prior distribution yields a global Bayes risk measure that provides an overall assessment of uncertainty.

Define the random variable X_β with density

$$f_\beta(t) = \frac{1}{\Gamma(\beta)} \Lambda^{\beta-1}(t) f(t), t > 0. \tag{3}$$

Under this prior structure, the Bayes risk coincides with the FGCRE:

$$\mathcal{E}_\beta(X) = \mathbb{E}(X_{\beta+1}) - \mathbb{E}(X_\beta),$$

as shown in Alomani and Kayid [14]. Moreover,

$$\frac{1}{\Gamma(\beta+1)} \mathbb{E}[X\Lambda^{\beta-1}(X)] = \frac{1}{\beta} \mathbb{E}(X_\beta).$$

Consequently, the deviation functional admits the equivalent representation

$$\mathbb{T}_\beta(\mathrm{F}) = \frac{\beta+1}{\beta} \mathbb{E}(\mathrm{X}_\beta) - \mathbb{E}(\mathrm{X}_{\beta+1}),\ \beta > 0. \tag{4}$$

2.4. Structural properties of the proposed functional

The functional $\mathbb{T}_\beta(F)$ satisfies:

1) $\mathbb{T}_\beta(F) \geq 0$ for all IFR distributions.

2) $\mathbb{T}_\beta(F) = 0$ if and only if $F \in \mathcal{C}$.

3) Empirically, $\mathbb{T}_\beta(F)$ tends to increase as the departure from exponentiality within IFR alternatives becomes more pronounced.

These properties make $\mathbb{T}_\beta(F)$ a natural basis for testing H_0 against IFR alternatives.

Proposition 2.1. (Strict positivity under strict IFR)

Assume F is absolutely continuous with hazard rate $\lambda(\cdot)$. If F is strictly IFR, i.e., $\lambda(t)$ is strictly increasing on $(0,\infty)$, then for every $\beta > 0$,

$$T_\beta(F) > 0.$$

Consequently, the scale-free functional $T_\beta^*(F) = T_\beta(F)/\mu$ is also strictly positive.

Proof. Recall that

$$\delta(t) = \int_0^t [\lambda(t) - \lambda(s)]ds = t\lambda(t) - \Lambda(t), t > 0,$$

and under IFR one has $\delta(t) \geq 0$, with equality identically if and only if $\lambda(\cdot)$ is constant (i.e., $F \in \mathcal{C}$). If $\lambda(\cdot)$ is strictly increasing, then for each fixed $t > 0$, I have $\lambda(t) > \lambda(s)$ for all $s \in [0,t)$. Hence the integrand is strictly positive on a set of positive Lebesgue measure, implying

$$\delta(t) > 0, \qquad \text{for all } t > 0.$$

Moreover, the weight

$$w_\beta(t) = \frac{\bar{F}(t)\Lambda^{\beta-1}(t)}{\Gamma(\beta+1)}, \qquad t > 0, \beta > 0$$

is nonnegative and is strictly positive for all t such that $\bar{F}(t) > 0$ and $\Lambda(t) > 0$.

Therefore, since

$$T_\beta(F) = \int_0^\infty w_\beta(t)\delta(t)dt,$$

I obtain $T_\beta(F) > 0$ because the integrand is strictly positive on a set of positive measure. This proves the claim.

Corollary 2.1. (Characterization of Exponentiality)

Let F be absolutely continuous with hazard rate $\lambda(\cdot)$ and suppose F is IFR. For any $\beta > 0$,

$$T_\beta(F) = 0 \iff F \in \mathcal{C}.$$

In other words, within the IFR class, the deviation functional $T_\beta(F)$ vanishes if and only if the hazard rate is constant, i.e., if and only if F is exponential.

Proof. If $F \in \mathcal{C}$, then $\lambda(t) \equiv \theta$ is constant, implying $\delta(t) = 0$ for all $t > 0$. Consequently, $T_\beta(F) = 0$. Conversely, assume F is IFR and $T_\beta(F) = 0$. Since

$$T_\beta(F) = \int_0^\infty w_\beta(t)\delta(t)dt,$$

with $w_\beta(t) \geq 0$ and $\delta(t) \geq 0$ under IFR, the integral can vanish only if $\delta(t) = 0$ almost everywhere. This implies

$$t\lambda(t) - \Lambda(t) = 0, t > 0,$$

which yields $\lambda(t) = \Lambda(t)/t$. Differentiating both sides shows that $\lambda'(t) = 0$ for all $t > 0$, so the hazard rate is constant. Hence, $F \in \mathcal{C}$.

Proposition 2.2. (Monotonicity in β under H_0)

If $F \in \mathcal{C}$ (i.e., F is exponential), then

$$T_\beta(F) = 0 \text{ for all } \beta > 0.$$

Consequently, the mapping $\beta \mapsto T_\beta(F)$ is constant (hence, nondecreasing and nonincreasing) on $(0, \infty)$ under H_0. The same conclusion holds for the scale-free version $T_\beta^*(F)$.

Proof. If $F \in \mathcal{C}$, then the hazard rate is constant, $\lambda(t) \equiv \theta$. Hence,

$$\delta(t) = \int_0^t [\lambda(t) - \lambda(s)]ds \equiv 0, t > 0.$$

Therefore,

$$T_\beta(F) = \int_0^\infty w_\beta(t)\delta(t)dt = 0 \text{ for all } \beta > 0,$$

which proves the result.

2.5. L-statistic representation

The functional can be expressed as

$$\mathbb{T}_\beta(F) = \int_0^\infty xJ_\beta\big(F(x)\big)dF(x), \tag{5}$$

where

$$J_\beta(u) = \frac{(-\log(1-u))^{\beta-1}}{\Gamma(\beta+1)}[\beta + 1 + \log(1-u)], \text{for all } 0 < u < 1. \tag{6}$$

Thus, $\mathbb{T}_\beta(F)$ belongs to the class of L-functionals.

2.6. Sample version

Let $X_{1:n} < X_{2:n} < \cdots < X_{n:n}$ denote the order statistics and F_n the empirical distribution function. The empirical analogue is

$$\hat{\mathbb{T}}_\beta = \mathbb{T}_\beta(F_n) = \int_0^\infty x J_\beta(F_n(x)) dF_n(x)$$

$$= \frac{1}{n}\sum_{i=1}^n J_\beta\left(\frac{i}{n}\right) X_{(i)} \tag{7}$$

Hence, $\hat{\mathbb{T}}_\beta$ is an L-statistic. To remove scale dependence, define the normalized statistic

$$\mathbb{T}_\beta^\star(F) = \frac{\mathbb{T}_\beta(F)}{\mu},$$

and its empirical counterpart

$$\hat{\mathbb{T}}_\beta^\star = \frac{\hat{\mathbb{T}}_\beta}{\bar{X}}, \tag{8}$$

where $\bar{X}$ is the sample mean. Large values of the test statistic $\hat{\mathbb{T}}_\beta^\star$ indicate a substantial departure from the exponential family in the direction of IFR behavior, thereby providing evidence against the null hypothesis H_0 and in support of the alternative $H_1: F \in \text{IFR} \setminus \mathcal{C}$. Consequently, the proposed test rejects H_0 at significance level α whenever $\hat{\mathbb{T}}_\beta^\star > c_\alpha$, where c_α is the $(1-\alpha)$-quantile of the null distribution of $\hat{\mathbb{T}}_\beta^\star$.

3. Exact finite-sample and asymptotic distribution under exponentiality

In this section, I derive the exact finite-sample null distribution of the proposed statistic and establish its asymptotic behavior. The exact distribution is obtained by expressing the statistic as a ratio of linear combinations of normalized spacings, thereby placing it within the classical L-statistic framework.

3.1. Exact finite-sample Null distribution

Under the null hypothesis $H_0: F \in \mathcal{C}$. Suppose that $X_1, X_2, \ldots, X_n$ are i.i.d. exponential with rate $\theta > 0$. The order statistics admit the well-known representation

$$X_{(r)} = \frac{1}{\theta}\sum_{j=1}^r \frac{E_j}{n-j+1}, r = 1, \ldots, n,$$

where $E_1, E_2, \ldots, E_n$ are i.i.d. standard exponential random variables.

Define the normalized spacings by

$$D_r = (n-r+1)\left(X_{(r)} - X_{(r-1)}\right), \qquad r = 1, \ldots, n,$$

with the convention $X_{(0)} = 0$. Under H_0, the variables $D_1, D_2, \ldots, D_n$ are i.i.d. exponential with rate θ, and $\sum_{r=1}^{n} D_r = n\bar{X}$.

By algebraic manipulation of the L-statistic representation, the normalized test statistic can be written as

$$\hat{\mathbb{T}}_{\beta}^{\star} = \frac{\sum_{r=1}^{n} b_{r,n} D_r}{\sum_{r=1}^{n} D_r}, \tag{9}$$

where the coefficients $b_{r,n}$ are given by

$$b_{r,n} = \frac{1}{n-r+1} \sum_{i=r}^{n} J_{\beta}\left(\frac{i}{n}\right), \text{ for all } r = 1, \ldots, n.$$

This representation expresses the statistic as a ratio of linear forms in independent exponential variables, which enables direct application of classical distribution theory. Throughout this section, I adopt the rate parameterization of the exponential distribution. That is, I assume that $X \sim \text{Exp}(\theta)$ with probability density function $f(x) = \theta e^{-\theta x}, \theta > 0$. Applying Theorem 2.4 from Box [17], which provides key results on the distribution of ratios and linear forms of independent exponential variates in the context of quadratic forms and variance component analysis, I immediately obtain the exact (finite sample) null distribution of $\hat{\mathbb{T}}_{\beta}^{\star}$ given by the following theorem.

Theorem 3.1. (Exact Null distribution)

Let $X_1, X_2, \ldots, X_n$ be i.i.d. exponential with distribution $F(x) = 1 - e^{-\frac{x}{2}}$, $x > 0$. Without loss of generality, I fix θ = 1/2 for convenience, since the statistic is scale invariant. Then, under H_0, the exact distribution of $\hat{\mathbb{T}}_{\beta}^{\star}$ is given by

$$\mathbb{P}\left(\hat{\mathbb{T}}_{\beta}^{\star} \leq x\right) = 1 - \sum_{\ell=1}^{n} \left[\prod_{\substack{m=1 \\ m \neq \ell}}^{n} \frac{b_{\ell,n} - x}{b_{\ell,n} - b_{m,n}}\right] \mathbb{I}\left(x \leq b_{\ell,n}\right), \tag{10}$$

provided that the coefficients $b_{1,n}, b_{2,n}, \ldots, b_{n,n}$ are pairwise distinct.

Proof. Given that $\sum_{r=1}^{n} D_r = \sum_{r=1}^{n} X_{(r)}$, the test statistic $\hat{\mathbb{T}}_{\beta}^{\star}$ can be expressed in terms of normalized spacings, as given in (9). This is derived from the relationship $n\hat{\mathbb{T}}_{\beta} = \sum_{r=1}^{n} b_{r,n} D_r$, which can be established by substituting the definition of $\hat{\mathbb{T}}_{\beta}^{\star}$ into the expression for $\hat{\mathbb{T}}_{\beta}$:

$$
\begin{aligned}
n\hat{\mathbb{I}}_\beta &= \sum_{r=1}^{n} b_{r,n} D_r = \sum_{r=1}^{n} b_{r,n}(n-r+1)\big(X_{(r)} - X_{(r-1)}\big) \\
&= \sum_{r=1}^{n} \big(X_{(r)} - X_{(r-1)}\big) \sum_{i=r}^{n} J_\beta\left(\frac{i}{n}\right) \\
&= \sum_{i=1}^{n} J_\beta\left(\frac{i}{n}\right) \sum_{r=1}^{i} \big(X_{(r)} - X_{(r-1)}\big) \\
&= \sum_{i=1}^{n} J_\beta\left(\frac{i}{n}\right) X_{(i)}.
\end{aligned}
$$

By equating the coefficients of $X_{(i)}$ on both sides and utilizing the relation between order statistics and spacings, I can derive:

$$
b_{r,n} = \frac{1}{n-r+1} \sum_{i=r}^{n} J_\beta\left(\frac{i}{n}\right), \text{for } r = 1,2,\dots,n.
$$

Since the coefficients $b_{r,n}$ are deterministic and pairwise distinct, the assumptions of Box [17] Theorem 2.4 are satisfied. Under H_0, note that each X_i follows an exponential distribution. The specific choice of $F(x) = 1 - e^{-x/2}$ indicates that $X_i \overset{d}{=} \chi_2^2$, which means each follows a chisquare distribution with 2 degrees of freedom. Consequently, the spacings $D_1, D_2, \dots, D_n$ are i.i.d. as χ_2^2. Applying Theorem 2.4 from Box [16] with $g_i = 1, v_i = 2$, and $s = 1$, I find:

$$
\mathbb{P}\big[\hat{\mathbb{I}}_\beta^\star \le x\big] = 1 - \mathbb{P}\left[\frac{\sum_{r=1}^{n} b_{r,n} D_r}{\sum_{r=1}^{n} D_r} > x\right] = 1 - \mathbb{P}\left[\sum_{r=1}^{n} \big(b_{r,n} - x\big) D_r > 0\right].
$$

The final probability represents the survival function of a linear combination of independent chi-square variables. By using the result from Box [17], I can express this as:

$$
\mathbb{P}\big[\hat{\mathbb{I}}_\beta^\star \le x\big] = 1 - \sum_{r=1}^{n} \left[\prod_{\substack{m=1 \\ m \ne r}}^{n} \frac{b_{r,n} - x}{b_{r,n} - b_{m,n}}\right] \mathbb{I}(\mathrm{x} \le b_{r,n}),
$$

thus completing the proof.

Remark 3.1. For fixed $\beta > 0$ and finite n, the coefficients $b_{r,n}, r = 1, \dots, n$, are strictly ordered. Indeed, these coefficients are defined through the score function $J_\beta(u)$ evaluated at the points $u_r = \frac{r}{n+1}$, which are strictly increasing in r. Since $J_\beta(u)$ is strictly monotone on $(0,1)$, it follows that the sequence $b_{r,n} = J_\beta(u_r)$ is strictly monotone in r. In particular, if $r \ne s$, then $b_{r,n} \ne b_{s,n}$, and hence the coefficients are pairwise distinct. This property guarantees that the exact distribution formula in Theorem 3.1 is well defined.

Remark 3.2. (Distribution-Freeness)

Although the theorem is stated for $\theta = 1/2$, the exact distribution holds for any $\theta > 0$. This follows from the scale invariance of

$$\hat{\mathbb{T}}_{\beta}^{\star} = \frac{\sum_{r=1}^{n} b_{r,n} D_r}{\sum_{r=1}^{n} D_r}.$$

Hence, the null distribution is distribution-free within the exponential family. The exact null distribution is computationally stable for moderate sample sizes ($n \leq 100$) and can be evaluated directly without numerical integration.

3.2. Asymptotic distribution

I now establish asymptotic normality. The following result follows from the general theory of L-statistics (Stigler [18]).

Theorem 3.2. (Asymptotic normality of $\hat{\mathbb{T}}_{\beta}$)

Let X be nonnegative with finite second moment and finite asymptotic variance $\sigma^2(J_\beta, F)$. Then, as $n \to \infty$,

$$\sqrt{n}\frac{\hat{\mathbb{T}}_{\beta} - \mu(J_\beta, F)}{\sigma(J_\beta, F)} \xrightarrow{d} N(0,1),$$

where

$$\mu(J_\beta, F) = \int_0^{\infty} x J_\beta(F(x)) dF(x),$$

and

$$\sigma^2(J_\beta, F) = \int_0^{\infty} \int_0^{\infty} J_\beta(F(x)) J_\beta(F(y)) \left[F(\min(x,y)) - F(x)F(y)\right] dxdy. \tag{11}$$

Here, $J_\beta(\cdot)$ denotes the score function defined in (6).

Combining Theorem 3.2 with Slutsky's theorem yields the asymptotic distribution of the scale-invariant statistic.

Theorem 3.3. (Asymptotic distribution of $\hat{\mathbb{T}}_{\beta}^{\star}$)

Under the conditions of Theorem 3.2,

$$\sqrt{n}\left(\hat{\mathbb{T}}_{\beta}^{\star} - \frac{\mathbb{T}_\beta(F)}{\mathbb{E}[X]}\right) \xrightarrow{d} N\left(0, \frac{\sigma^2(J_\beta, F)}{(\mathbb{E}[X])^2}\right).$$

Asymptotic behavior under H_0

Under exponentiality, without loss of generality assume $F(x) = 1 - e^{-x}$ for $x > 0$. Then, $\mathbb{T}_\beta(F) = 0$ and $\mathbb{E}[X] = 1$. Hence

$$\sqrt{n}\hat{\mathbb{T}}_\beta^\star \xrightarrow{d} N\left(0, \sigma^2(J_\beta, F)\right).$$

Thus, large positive values provide evidence of IFR behavior.

Variance estimation

Following Jones and Zitikis [19], a consistent estimator of the asymptotic variance is:

$$\hat{\sigma}^2(J_\beta, F_n) = \sum_{i=1}^{n-1} \sum_{j=1}^{n-1} \left(\min\left(\frac{i}{n}, \frac{j}{n}\right) - \frac{ij}{n^2}\right) J_\beta\left(\frac{i}{n}\right) J_\beta\left(\frac{j}{n}\right) \Delta_i \Delta_j, \tag{12}$$

where $\Delta_i = X_{(i+1)} - X_{(i)}$.

The large-sample test rejects H_0 at level α whenever

$$\frac{\sqrt{n}\hat{\mathbb{T}}_\beta^\star}{\hat{\sigma}(J_\beta, F_n)} > z_{1-\alpha}. \tag{13}$$

4. Simulation study

In this section, I examine the finite-sample performance of the proposed statistic $\hat{T}_\beta^*$ through a comprehensive Monte Carlo study. My primary objective is to assess its empirical power against a range of IFR alternatives and to evaluate the influence of the tuning parameter β on detection sensitivity. Although an exact finite-sample null distribution is derived, its direct evaluation involves numerically intensive computations, particularly for moderate and large sample sizes. Consequently, Monte Carlo simulation is employed to obtain accurate approximations of the critical values in a computationally efficient manner. This strategy is standard in similar settings where exact distributions are theoretically available but practically difficult to evaluate. All reported results are based on a sufficiently large number of replications to ensure numerical stability and precision. For comparison purposes, I include several well-known tests for exponentiality against IFR alternatives, including tests based on normalized spacings, U-statistics, moment inequalities, and total time on test transforms.

Alternative models

I consider three parametric families that are widely used in reliability engineering and survival analysis and that represent progressively increasing departures from exponentiality:

- Linear Failure Rate (LFR) distribution, which includes the exponential and Rayleigh models as special cases and provides a natural framework for modeling linear aging mechanisms;
- Makeham distribution, commonly employed in survival and demographic modeling due to its flexible hazard structure;
- Weibull distribution, the classical model for monotone aging behavior and one of the most fundamental lifetime distributions in reliability analysis.

These families enable me to investigate the behavior of the proposed test under IFR mechanisms. Table 1 summarizes the corresponding distributional forms.

Table 1. Cumulative distribution function with the scale parameter θ.

Distribution	Survival function	Support
LFR	$\bar{F}_1(x) = e^{-(x+0.5\theta x^2)}$,	$x > 0, \theta > 0$
Makeham	$\bar{F}_2(x) = e^{-(x+\theta(x+e^{-x}-1))}$,	$x > 0, \theta > 0$
Weibull	$\bar{F}_3(x) = e^{-x^\theta}$,	$x > 0, \theta > 0$

Simulation design

A central aspect of this study is to investigate how the tuning parameter β affects the power of the test. Since $\hat{T}_\beta^*$ is scale-invariant, the rejection region depends only on the shape of the underlying distribution, not on its scale parameter. This property enables meaningful comparisons across models without additional normalization. For each sample size n, critical values are obtained via Monte Carlo simulation under the null hypothesis of exponentiality. Specifically,

(i). Generate 10,000 independent samples from the standard exponential distribution;

(ii). Compute $\hat{T}_\beta^*$ for each sample;

(iii). Use the empirical $(1-\alpha)$-quantile as the critical value at significance level α.

For baseline calibration, I focus on $n = 25$, and denote the resulting critical value by $\hat{T}^*_{\beta,(1-\alpha)}$. I note that additional experiments confirm stability of the null quantiles across other sample sizes. The null hypothesis is rejected at level $\alpha = 0.05$ whenever $\hat{T}_\beta^* > \hat{T}^*_{\beta,(0.95)}$.

Power estimation

Empirical power is estimated using 5,000 simulated samples from each alternative distribution across a range of parameter values. For each configuration, power is computed as the proportion of rejections. This framework enables me to:

(i). Evaluate sensitivity of the proposed statistic to varying degrees of IFR departure;

(ii). Compare performance across aging mechanisms;

(iii). Identify values of β that maximize power under specific alternatives.

The results provide two key insights:

1) The proposed entropy-based test exhibits strong and stable power across all three IFR families, with power increasing monotonically as sample size grows, confirming consistency.

2) Tuning parameter β plays a substantive role in shaping detection performance. Moderate values of β tend to offer balanced sensitivity across alternatives, whereas larger values may enhance detection under stronger aging effects. This adaptability distinguishes the proposed family from classical single statistic procedures.

Tables 2–4 report the empirical power comparisons of the competing procedures at significance level $\alpha = 0.05$ under the LFR, Makeham, and Weibull alternatives, respectively. Collectively, these results demonstrate a consistent increase in power as the departure from exponentiality becomes more pronounced across all three distributional families. For moderate deviations, where discrimination is statistically most demanding, the proposed entropy-based statistic exhibits competitive and often superior performance relative to the tests. The adaptability introduced through tuning parameter β is reflected in the results, as certain values yield enhanced sensitivity depending on underlying aging mechanism. Under stronger departures, power approaches unity across most procedures, particularly in the Weibull case, where the IFR structure becomes increasingly pronounced.

Table 2. Power comparisons of the tests for the LFR distribution at significance level $\alpha = 0.05$.

Sample size	θ	$\hat{\mathbb{T}}^{\star}_{0.2}$	$\hat{\mathbb{T}}^{\star}_{0.4}$	$\hat{\mathbb{T}}^{\star}_{0.6}$	$\hat{\mathbb{T}}^{\star}_{0.8}$	$\hat{\mathbb{T}}^{\star}_{1.0}$	$\hat{\mathbb{T}}^{\star}_{1.2}$	$\hat{\mathbb{T}}^{\star}_{1.4}$	$\hat{\mathbb{T}}^{\star}_{1.6}$	$\hat{\mathbb{T}}^{\star}_{1.8}$
	1.2	0.2810	0.2918	0.3080	0.3272	0.3328	0.3212	0.2900	0.2232	0.1556
	1.5	0.3172	0.3454	0.3536	0.3658	0.3852	0.3702	0.3268	0.2666	0.1602
$n = 20$	2.0	0.3790	0.3870	0.4254	0.4740	0.4224	0.4080	0.3650	0.3066	0.1762
	2.5	0.4122	0.4636	0.4560	0.4714	0.4684	0.4554	0.4016	0.3496	0.2018
	3.0	0.4408	0.4872	0.5086	0.5098	0.5098	0.4830	0.4524	0.3716	0.1902
	1.2	0.3850	0.4362	0.4370	0.4616	0.4346	0.4256	0.4078	0.3628	0.2546
	1.5	0.4534	0.4738	0.5222	0.5186	0.5130	0.5134	0.4730	0.4178	0.3214
$n = 30$	2.0	0.5152	0.5482	0.5848	0.6264	0.5796	0.5476	0.5472	0.4138	0.3486
	2.5	0.5844	0.6172	0.6672	0.6644	0.6646	0.6472	0.6256	0.5072	0.3716
	3.0	0.6076	0.6506	0.6896	0.6978	0.6852	0.6788	0.6196	0.5376	0.4042
	1.2	0.4944	0.5040	0.5304	0.5754	0.6038	0.5748	0.5418	0.4650	0.3752
	1.5	0.5164	0.6014	0.6486	0.6404	0.6518	0.6452	0.6158	0.5096	0.4082
$n = 40$	2.0	0.6310	0.6894	0.7210	0.7408	0.7218	0.7226	0.6400	0.6098	0.5062
	2.5	0.6914	0.7344	0.7948	0.7968	0.7902	0.7442	0.7140	0.6418	0.5006
	3.0	0.7368	0.8102	0.8266	0.8382	0.8390	0.8124	0.7632	0.6732	0.5588
	1.2	0.5730	0.6244	0.6768	0.6836	0.6778	0.6702	0.6194	0.5660	0.4756
	1.5	0.6364	0.6838	0.7198	0.7380	0.7570	0.7240	0.6964	0.6162	0.5326
$n = 50$	2.0	0.7038	0.7844	0.8110	0.8202	0.8430	0.8156	0.7820	0.7134	0.5830
	2.5	0.7836	0.8494	0.8692	0.8732	0.8818	0.8556	0.8164	0.7578	0.6546
	3.0	0.8260	0.8742	0.9102	0.9088	0.9052	0.8936	0.8522	0.7874	0.6562

Table 3. Power comparisons of the tests for the Makeham distribution at significance level $\alpha = 0.05$.

Sample size	θ	$\hat{\mathbb{T}}^{\star}_{0.2}$	$\hat{\mathbb{T}}^{\star}_{0.4}$	$\hat{\mathbb{T}}^{\star}_{0.6}$	$\hat{\mathbb{T}}^{\star}_{0.8}$	$\hat{\mathbb{T}}^{\star}_{1.0}$	$\hat{\mathbb{T}}^{\star}_{1.2}$	$\hat{\mathbb{T}}^{\star}_{1.4}$	$\hat{\mathbb{T}}^{\star}_{1.6}$	$\hat{\mathbb{T}}^{\star}_{1.8}$
$n = 20$	1.2	0.1802	0.1806	0.2034	0.1910	0.1712	0.1722	0.1664	0.1272	0.0904
	1.5	0.2140	0.2192	0.2286	0.2434	0.2302	0.1964	0.1842	0.1750	0.1146
	2.0	0.2652	0.2822	0.2832	0.2972	0.2554	0.2458	0.2372	0.2086	0.1094
	2.5	0.3090	0.3068	0.3066	0.3264	0.3336	0.3088	0.2720	0.2188	0.1336
	3.0	0.3406	0.3710	0.3832	0.3522	0.3528	0.3158	0.3130	0.2318	0.1418
$n = 30$	1.2	0.2430	0.2756	0.2630	0.2690	0.2776	0.2222	0.2168	0.1918	0.1474
	1.5	0.2860	0.3072	0.3250	0.3164	0.3022	0.2806	0.2520	0.2234	0.1524
	2.0	0.3410	0.3782	0.3852	0.3796	0.3622	0.3480	0.3248	0.2578	0.1826
	2.5	0.4192	0.4496	0.4520	0.4442	0.4000	0.3810	0.3712	0.2750	0.2010
	3.0	0.4798	0.4900	0.4968	0.5174	0.4856	0.4594	0.4146	0.3300	0.2218
$n = 40$	1.2	0.3014	0.3248	0.3104	0.3358	0.3174	0.2962	0.2436	0.2434	0.1768
	1.5	0.3520	0.3828	0.4060	0.3746	0.3772	0.3604	0.3484	0.2758	0.1988
	2.0	0.4424	0.4868	0.4982	0.4886	0.4850	0.4216	0.4142	0.3332	0.2610
	2.5	0.5128	0.5726	0.5732	0.5724	0.5236	0.5214	0.4450	0.3796	0.3066
	3.0	0.5546	0.6004	0.6076	0.6310	0.6192	0.5194	0.5018	0.4226	0.3112
$n = 50$	1.2	0.3474	0.3548	0.3774	0.3584	0.3530	0.3384	0.3096	0.2516	0.2192
	1.5	0.4496	0.4596	0.4718	0.4666	0.4198	0.3908	0.3516	0.2920	0.2624
	2.0	0.5226	0.5442	0.5598	0.5696	0.5554	0.5106	0.4542	0.4204	0.3066
	2.5	0.5972	0.6438	0.6544	0.6454	0.6294	0.5868	0.5452	0.4636	0.3572
	3.0	0.6912	0.7180	0.7312	0.7202	0.6978	0.6480	0.5836	0.5326	0.4130

Table 4. Power comparisons of the tests for the Weibull distribution at significance level $\alpha = 0.05$.

Sample size	θ	$\hat{\mathbb{T}}^{\star}_{0.2}$	$\hat{\mathbb{T}}^{\star}_{0.4}$	$\hat{\mathbb{T}}^{\star}_{0.6}$	$\hat{\mathbb{T}}^{\star}_{0.8}$	$\hat{\mathbb{T}}^{\star}_{1.0}$	$\hat{\mathbb{T}}^{\star}_{1.2}$	$\hat{\mathbb{T}}^{\star}_{1.4}$	$\hat{\mathbb{T}}^{\star}_{1.6}$	$\hat{\mathbb{T}}^{\star}_{1.8}$
$n = 20$	1.2	0.2254	0.2086	0.2192	0.2028	0.2066	0.1758	0.1592	0.1158	0.0904
	1.5	0.6612	0.6736	0.6646	0.6478	0.5710	0.5608	0.4560	0.2984	0.1296
	2.0	0.9772	0.9860	0.9858	0.9812	0.9714	0.9556	0.8770	0.7154	0.1640
	2.5	1.0000	0.9998	0.9998	0.9998	1.0000	0.9986	0.9936	0.9066	0.1176
	3.0	1.0000	1.0000	1.0000	1.0000	1.0000	1.0000	1.0000	0.9814	0.0922
$n = 30$	1.2	0.2858	0.3090	0.3128	0.2714	0.2596	0.2328	0.1904	0.1668	0.1126
	1.5	0.8324	0.8580	0.8312	0.8028	0.7718	0.7004	0.6192	0.5012	0.3032
	2.0	0.9994	0.9988	0.9998	0.9986	0.9986	0.9922	0.9832	0.9180	0.6070
	2.5	1.0000	1.0000	1.0000	1.0000	1.0000	1.0000	0.9998	0.9950	0.8346
	3.0	1.0000	1.0000	1.0000	1.0000	1.0000	1.0000	1.0000	1.0000	0.8992
$n = 40$	1.2	0.3822	0.3854	0.3552	0.3230	0.3292	0.2706	0.2520	0.2350	0.1592
	1.5	0.9262	0.9320	0.9196	0.9146	0.8524	0.8334	0.7464	0.6486	0.4616
	2.0	0.9994	1.0000	1.0000	1.0000	1.0000	0.9996	0.9968	0.9808	0.8668
	2.5	1.0000	1.0000	1.0000	1.0000	1.0000	1.0000	1.0000	1.0000	0.9840
	3.0	1.0000	1.0000	1.0000	1.0000	1.0000	1.0000	1.0000	1.0000	0.9988
$n = 50$	1.2	0.4556	0.4664	0.4174	0.3944	0.3516	0.3374	0.2898	0.2592	0.2020
	1.5	0.9740	0.9726	0.9684	0.9622	0.9402	0.8956	0.8382	0.7550	0.6044
	2.0	1.0000	1.0000	1.0000	1.0000	1.0000	1.0000	0.9996	0.9952	0.9568
	2.5	1.0000	1.0000	1.0000	1.0000	1.0000	1.0000	1.0000	1.0000	0.9990
	3.0	1.0000	1.0000	1.0000	1.0000	1.0000	1.0000	1.0000	1.0000	1.0000

To assess the relative performance of the proposed test statistic $\hat{\mathbb{T}}^{\star}_{\beta}$ under IFR alternatives, I compare its empirical power against a selection of established nonparametric tests from the literature. These competing procedures, each designed to test exponentiality against IFR alternatives, are grounded in methodological frameworks, including spacings, U-statistics, L-statistics, and stochastic orderings. A common feature among them is scale invariance, asymptotic normality, and consistency under IFR alternatives. A brief description of each test, including its test statistic and underlying methodology, is provided below. These procedures leverage a variety of statistical constructs such as normalized spacings, U-statistics, L-statistics, and stochastic orderings and are typically designed to be scale-invariant, asymptotically normal, and consistent under the IFR class. The key competitors considered in this study are summarized as follows:

- Klefsjö [8] introduced the scale-invariant statistic

$$A_1 = \frac{\sum_{j=1}^{n} \alpha_j D_j}{\sum_{j=1}^{n} D_j},$$

where $D_j = (n - j + 1)\left(X_{(j)} - X_{(j-1)}\right)$ are normalized spacings with $X_{(0)} = 0$, and

$$\alpha_j = \frac{(n+1)^3 j - 3(n+1)^2 j^2 + 2(n+1)j^3}{6}, j = 1,2, \ldots, n.$$

Negative values of A_1 provide evidence in favor of an IFR distribution.

- Ahmad [6] proposed an asymptotically normal and scale-invariant U-statistic:

$$A_2 = \frac{1}{n(n-1)} \sum_{i \neq j} \left\{ 2e^{-X_i} - e^{-X_i - X_j} - e^{-2\min(X_i, X_j)} - 2\min(X_i, X_j) e^{-\min(X_i, X_j)} \right\}.$$

- Ahmad et al. [20] derived a consistent, scale-invariant test based on a second-order moment inequality for IFR distributions:

$$A_3 = \frac{\hat{\delta}_1}{\bar{X}^2}, \text{ where } \hat{\delta}_1 = \frac{1}{n(n-1)} \sum_{i \neq j} \left\{ 2\min(X_i, X_j)^2 - X_i X_j \right\}.$$

- Mitra and Anis [10] proposed a test based on a linear combination of order statistics:

$$B_n = \frac{1}{n^2} \sum_{j=1}^{n} (2 + 3n - 4j) X_{(j)}.$$

The scale-invariant form is $A_4 = \frac{B_n}{\bar{X}}$, and the null hypothesis of exponentiality is rejected for large positive values of A_4.

- Ahmad [21] derived a moment inequality-based statistic:

$$A_5 = \frac{1}{\bar{X}^2} \left\{ \frac{2}{n(n-1)} \sum_{i<j} \left[\min(X_i^2, X_j^2) - \frac{X_i X_j}{2} \right] \right\},$$

which is consistent against IFR alternatives and invariant under scale transformations.

Collectively, these tests provide a rich toolkit for detecting departures from exponentiality in favor of IFR alternatives, each leveraging distinct probabilistic or analytic properties of the exponential and IFR classes.

The empirical power of the proposed test statistics is evaluated through Monte Carlo simulations based on 5,000 replications for sample sizes $n = 25, 50,$ and 100. For each replication, power is calculated as the proportion of cases in which the test statistic exceeds its critical value, with critical values determined under the null hypothesis of exponentiality at the 5% significance level. As expected, the power of all tests increases monotonically with sample size, thereby confirming their consistency. Across the range of alternative distributions considered, including LFR, Makeham, and Weibull models, the proposed statistic $\hat{\mathbb{T}}_\beta^*$, evaluated for selected values of β (e.g., $0.6, 0.8, 1.0$) demonstrates competitive performance and frequently surpasses tests such as A_1, A_2, A_3, A_4, and A_5, particularly for moderate to large sample sizes. This finding underscores the test's enhanced sensitivity to departures from exponentiality within the distribution families examined. For the Weibull alternative with shape parameter $\theta > 1$, a member of the IFR class $\hat{\mathbb{T}}_\beta^*$ exhibits relatively high power

even in small samples. Its power improves markedly as sample size increases, achieving near-perfect detection for Weibull and other IFR alternatives when $n = 100$. These results suggest that $\hat{\mathbb{T}}_{\beta}^{*}$ is particularly effective at identifying IFR behavior, especially in larger samples. Overall, the proposed statistic performs robustly alternatives, although its relative effectiveness depends on the alternative distribution and the sample size under consideration. These findings provide practical guidance for selecting tuning parameter β to maximize power against anticipated alternatives.

Tables 5–7 summarize the empirical power comparisons at significance level α=0.05 for increasing sample sizes $n = 25, 50,$ and 100, respectively. These results illustrate the improvement in detection capability as sample size increases. For moderate departures from exponentiality, where discrimination is statistically most demanding, the proposed entropy-based statistic consistently achieves competitive and often superior power across the LFR, Makeham, and Weibull alternatives. As the sample size grows, empirical power increases uniformly for all procedures, confirming the consistency established in Section 3. For stronger departures, power approaches unity at $n = 50$ and $n = 100$ and differences among methods naturally diminish. Nevertheless, the proposed test maintains stable and robust performance across all configurations. The influence of tuning parameter β is more pronounced in smaller samples and under moderate alternatives, while its relative impact decreases as sample size increases and discrimination becomes easier. Overall, Tables 5–7 collectively demonstrate that the proposed test family performs reliably across small, moderate, and large sample settings.

Table 5: Power comparisons of the tests at significance level $\alpha = 0.05$ and $n = 25$.

Distribution	θ	A_1	A_2	A_3	A_4	A_5	$\hat{\mathbb{T}}_{0.6}^{\star}$	$\hat{\mathbb{T}}_{0.8}^{\star}$	$\hat{\mathbb{T}}_{1.0}^{\star}$
	1.2	0.3200	0.1966	0.2560	0.3930	0.2690	0.3920	0.4338	0.3998
	1.5	0.3586	0.2110	0.2944	0.4228	0.3098	0.4582	0.4846	0.4456
LFR	2.0	0.4168	0.2022	0.3504	0.5100	0.3356	0.5220	0.5610	0.5158
	2.5	0.4414	0.2020	0.3758	0.5658	0.3922	0.5698	0.5992	0.5800
	3.0	0.5052	0.1922	0.4106	0.6066	0.4292	0.6224	0.6496	0.6164
	1.2	0.1788	0.1184	0.1508	0.2230	0.1472	0.2356	0.2478	0.2090
	1.5	0.2158	0.1180	0.1884	0.2672	0.1796	0.2754	0.2776	0.2484
Makeham	2.0	0.2508	0.1272	0.2230	0.3358	0.2218	0.3518	0.3594	0.2964
	2.5	0.2974	0.1288	0.2634	0.3726	0.2494	0.4024	0.4146	0.3538
	3.0	0.3254	0.1320	0.2842	0.4298	0.2864	0.4476	0.4638	0.3956
	1.2	0.1664	0.2006	0.1366	0.2480	0.1434	0.2396	0.2548	0.2232
	1.5	0.4380	0.5736	0.4172	0.7420	0.4086	0.7444	0.7544	0.6844
Weibull	2.0	0.8168	0.9638	0.8768	0.9950	0.8952	0.9972	0.9978	0.9914
	2.5	0.9504	0.9994	0.9958	1.0000	0.9958	1.0000	1.0000	1.0000
	3.0	0.9874	1.0000	1.0000	1.0000	0.9998	1.0000	1.0000	1.0000

Table 6. Power comparisons of the tests at significance level $\alpha = 0.05$ and $n = 50$.

Distribution	θ	A_1	A_2	A_3	A_4	A_5	$\hat{\mathbb{I}}^{\star}_{0.6}$	$\hat{\mathbb{I}}^{\star}_{0.8}$	$\hat{\mathbb{I}}^{\star}_{1.0}$
	1.2	0.5066	0.4112	0.5104	0.6520	0.5304	0.6368	0.6694	0.6664
	1.5	0.5794	0.4444	0.5738	0.7122	0.5978	0.7138	0.7422	0.7324
LFR	2.0	0.6542	0.4838	0.6568	0.7994	0.6834	0.8090	0.8294	0.8096
	2.5	0.7108	0.4912	0.7056	0.8564	0.7322	0.8576	0.8694	0.8584
	3.0	0.7436	0.4996	0.7500	0.8838	0.7730	0.8934	0.9152	0.9018
	1.2	0.2834	0.1924	0.2638	0.4028	0.2602	0.3732	0.3622	0.3564
	1.5	0.3336	0.2214	0.3128	0.4770	0.3004	0.4590	0.4328	0.4568
Makeham	2.0	0.4250	0.2562	0.3876	0.5780	0.3692	0.5648	0.5608	0.5472
	2.5	0.4836	0.2682	0.4506	0.6752	0.4468	0.6372	0.6430	0.6334
	3.0	0.5446	0.2746	0.5134	0.7230	0.4948	0.7034	0.7084	0.6956
	1.2	0.2846	0.2856	0.2012	0.4224	0.2028	0.4122	0.4054	0.3656
	1.5	0.7442	0.8348	0.6962	0.9658	0.6858	0.9686	0.9572	0.9418
Weibull	2.0	0.9788	0.9994	0.9968	1.0000	0.9972	1.0000	1.0000	1.0000
	2.5	0.9984	1.0000	1.0000	1.0000	1.0000	1.0000	1.0000	1.0000
	3.0	1.0000	1.0000	1.0000	1.0000	1.0000	1.0000	1.0000	1.0000

Table 7. Power comparisons of the tests at significance level $\alpha = 0.05$ and $n = 100$.

Distribution	θ	A_1	A_2	A_3	A_4	A_5	$\hat{\mathbb{I}}^{\star}_{0.6}$	$\hat{\mathbb{I}}^{\star}_{0.8}$	$\hat{\mathbb{I}}^{\star}_{1.0}$
	1.2	0.7794	0.6592	0.8192	0.9306	0.8424	0.9202	0.9426	0.9452
	1.5	0.8384	0.7166	0.8812	0.9568	0.8946	0.9610	0.9718	0.9694
LFR	2.0	0.8970	0.7766	0.9290	0.9818	0.9424	0.9830	0.9872	0.9880
	2.5	0.9276	0.7970	0.9516	0.9916	0.9628	0.9926	0.9954	0.9938
	3.0	0.9534	0.8020	0.9702	0.9960	0.9792	0.9952	0.9978	0.9986
	1.2	0.4726	0.3588	0.4204	0.6308	0.4372	0.6360	0.6068	0.5822
	1.5	0.5582	0.4132	0.5042	0.7240	0.5294	0.7356	0.7102	0.7110
Makeham	2.0	0.6664	0.4944	0.6282	0.8360	0.6424	0.8628	0.8318	0.8216
	2.5	0.7566	0.5226	0.7120	0.9100	0.7300	0.9126	0.9026	0.8918
	3.0	0.8040	0.5756	0.7846	0.9440	0.7970	0.9520	0.9434	0.9304
	1.2	0.4428	0.4804	0.3366	0.7080	0.3664	0.7062	0.6482	0.6052
	1.5	0.9330	0.9878	0.9532	0.9998	0.9542	0.9998	0.9996	0.9994
Weibull	2.0	0.9996	1.0000	1.0000	1.0000	1.0000	1.0000	1.0000	1.0000
	2.5	1.0000	1.0000	1.0000	1.0000	1.0000	1.0000	1.0000	1.0000
	3.0	1.0000	1.0000	1.0000	1.0000	1.0000	1.0000	1.0000	1.0000

Figures 1–3 display the empirical power function plots for the LFR, Makeham, and Weibull distributions, respectively. These graphical representations complement the numerical findings reported in Tables 2–4 by visually illustrating the monotonic increase in power as the departure from exponentiality becomes more pronounced. Across all three alternatives, the proposed entropy-based statistic exhibits stable and steadily increasing power curves, particularly in the moderate-deviation region where discrimination is most challenging. The influence of tuning parameter β is evident in the

relative positioning of the curves, confirming that different values of β enhance sensitivity under different aging mechanisms. For stronger departures, most notably under the Weibull alternative, the power curves rapidly approach unity for all procedures, reinforcing the consistency and effectiveness of the proposed method. Overall, Figures 1–3 provide clear graphical support for the robustness and competitive performance of the proposed test family.

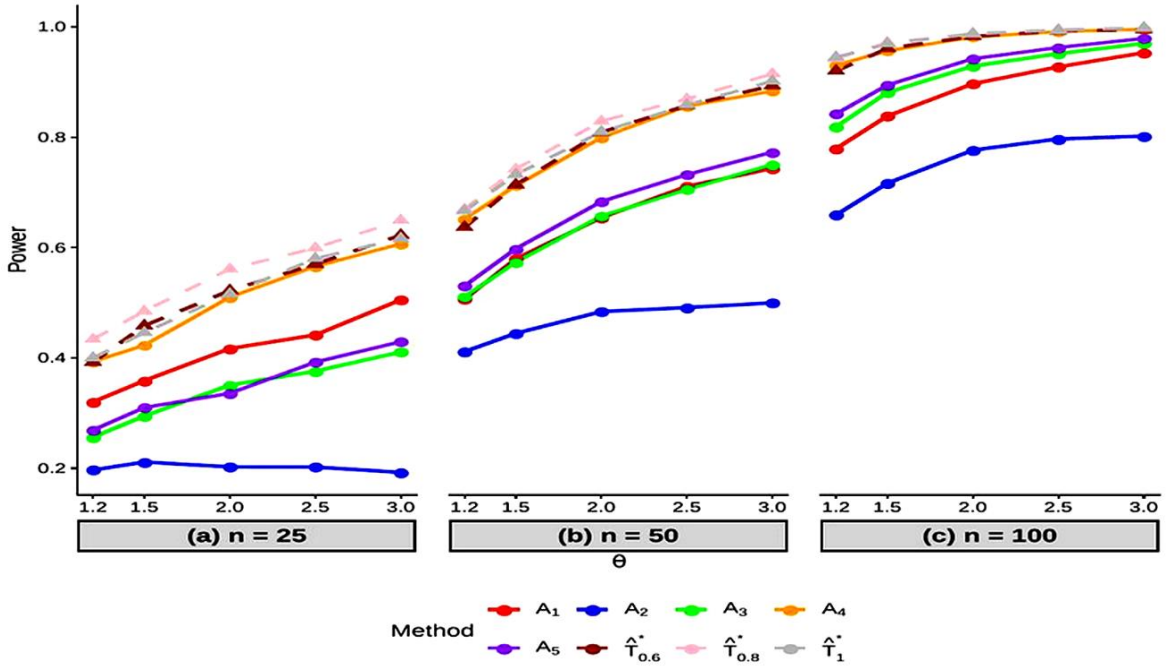

Figure 1. Empirical power function plots for LFR distribution.

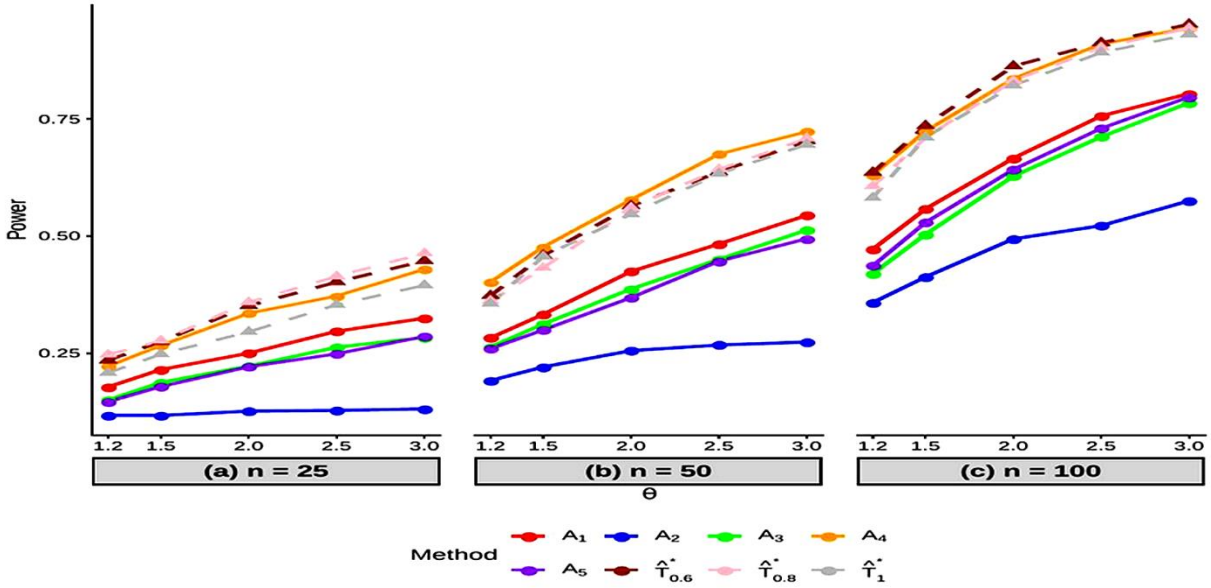

Figure 2. Empirical power function plots for Makeham distribution.

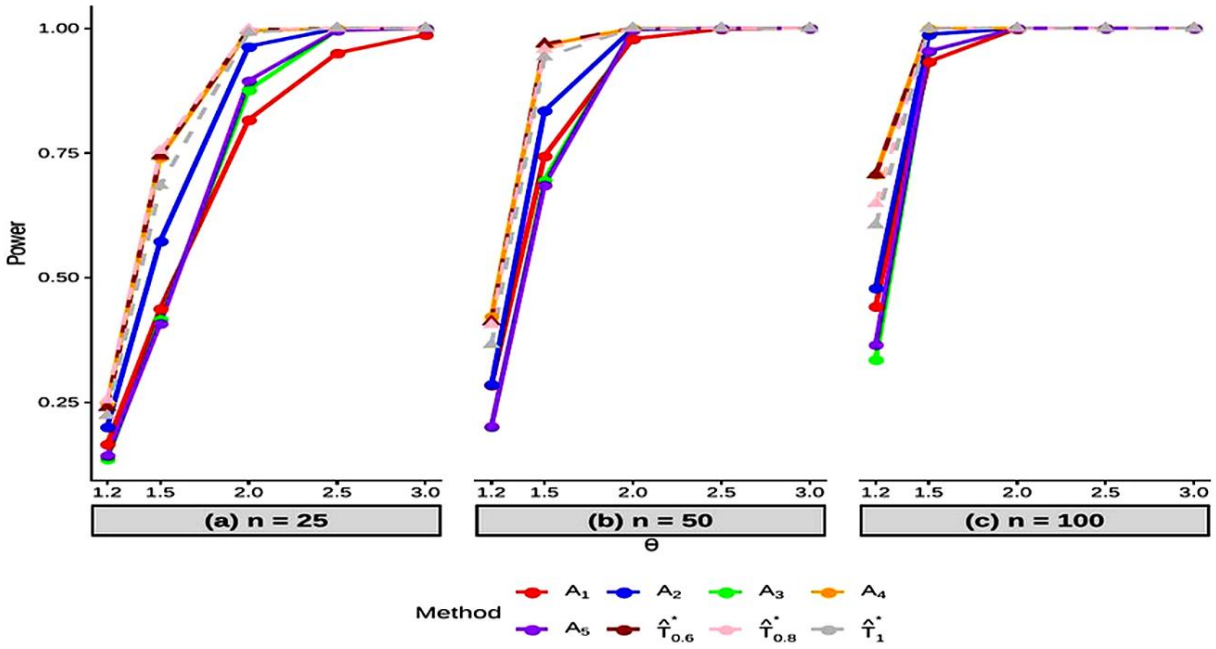

Figure 3. Empirical power function plots for Weibull distribution.

To further strengthen the empirical assessment, I supplement the numerical comparisons with a direct graphical comparison of the empirical power functions of the proposed test and several benchmark procedures commonly used in the literature for testing exponentiality against IFR alternatives. In particular, I consider representative competing methods based on normalized spacings, total time on test transforms, and moment-type statistics. This graphical comparison provides an immediate visual assessment of the relative sensitivity of the procedures under selected IFR alternatives and helps clarify the practical advantage of the proposed method across parameter settings.

The figure shows that the proposed method maintains strong and competitive power across the considered parameter values, particularly as the departure from exponentiality in the IFR direction becomes more pronounced. In addition, Figure 4 provides a direct visual comparison of the empirical power of the proposed test and several benchmark procedures under the Weibull alternative when n=50. The results show that the proposed method performs competitively across the full range of parameter values and exhibits particularly strong power as the deviation from exponentiality becomes more pronounced. This graphical evidence is consistent with the numerical findings reported in the corresponding tables and further supports the practical effectiveness of the proposed procedure.

The simulation results confirm that the proposed entropy-based test maintains strong sensitivity to moderate deviations from exponentiality, which are particularly critical in preventive maintenance planning. Misclassification of early-stage aging may lead to inefficient replacement strategies. Moreover, the stability of power as sample size increases further demonstrates robustness in realistic industrial reliability settings. The proposed test demonstrates stable size control and competitive power performance across all considered scenarios.

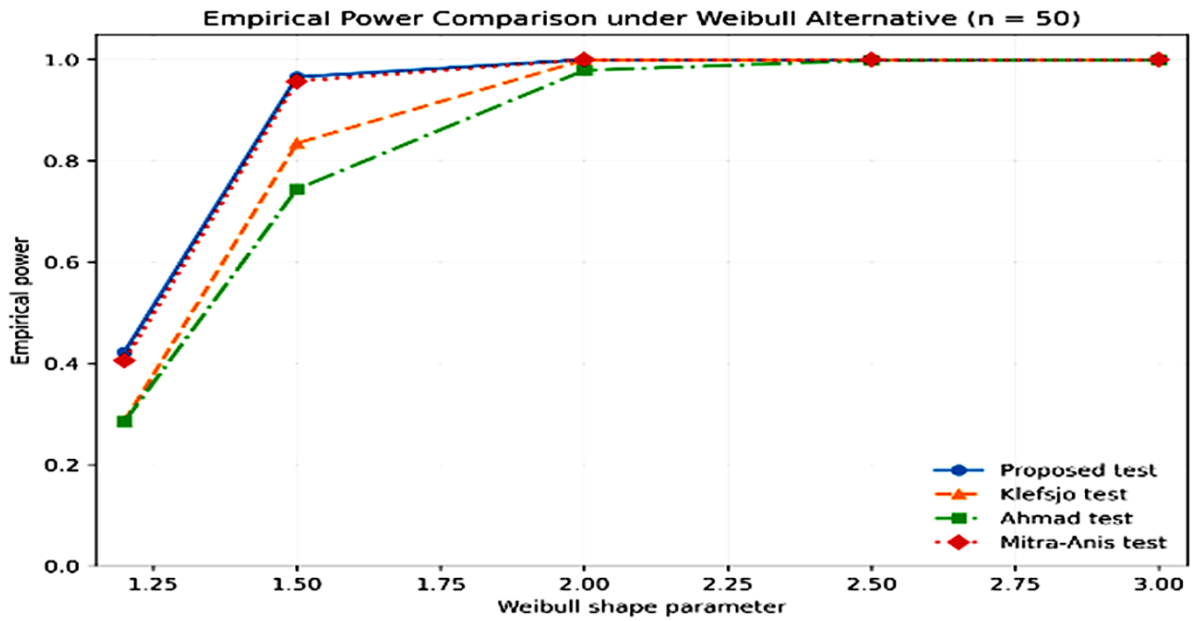

Figure 4. Empirical power comparison of the proposed test and selected benchmark procedures under the Weibull alternative for sample size n=50.

4.1. Real data example

To illustrate the practical applicability of the proposed statistic $\hat{\mathbb{T}}_{\beta}^{*}$, I analyze four real datasets drawn from reliability engineering and related applied domains. Prior to formal hypothesis testing, it is informative to conduct an exploratory graphical assessment of the failure rate behavior. For this purpose, I employ the TTT plot, originally introduced by Barlow and Campo [22], which is a standard diagnostic tool for identifying aging patterns. All numerical results reported in this section are presented with increased precision.

Let $X_{1:n} \leq X_{2:n} \leq \cdots \leq X_{n:n}$; the normalized spacing corresponding to the k-th failure is

$$D_k = (n-k+1)(X_{k:n} - X_{k-1:n}), k = 1, \ldots, n$$

where $X_{0:n} = 0$. The cumulative total time on test through the i-th failure is then computed as

$$S_i = \sum_{k=1}^{i} D_k, i = 1, \ldots, n$$

and $S_0 = 0$. The TTT plot is generated by plotting the coordinates $\left(\frac{i}{n}, \frac{S_i}{S_n}\right)$, for all $i = 0,1, \ldots, n$, and joining consecutive points with straight lines. As discussed, a TTT plot that closely follows the diagonal suggests exponentiality (constant failure rate), while a concave curve is indicative of an IFR distribution. By comparison, observations drawn from an IFR distribution generally yield a concave TTT plot, which is indicative of a progressively increasing failure rate. Consequently, this graphical tool provides a valuable initial indication of whether the IFR assumption appears reasonable, thereby

guiding the subsequent application of the more rigorous testing procedure based on $\hat{\mathbb{T}}_{\beta}^{*}$. For each dataset, I compute the test statistic for three representative values of the parameter $\beta(0.6, 0.8, \text{and } 1.0)$ and report the corresponding p -values.

Dataset 1: Aircraft air-conditioning failures

The first dataset, originally reported by Proschan [23], contains 30 failure times (in operating hours) of air-conditioning systems from a Boeing 720 aircraft. The observations are: 97, 51, 11, 4, 141, 18, 142, 68, 77, 80, 1, 16, 106, 206, 82, 54, 31, 216, 46, 111, 39, 63, 18, 191, 18, 163, 24, 11, 102, and 15.

Figure 5 presents the TTT plot with the Q–Q plot against the exponential distribution. The TTT curve closely follows the diagonal, and the Q–Q plot exhibits approximate linear alignment, indicating compatibility with exponentiality.

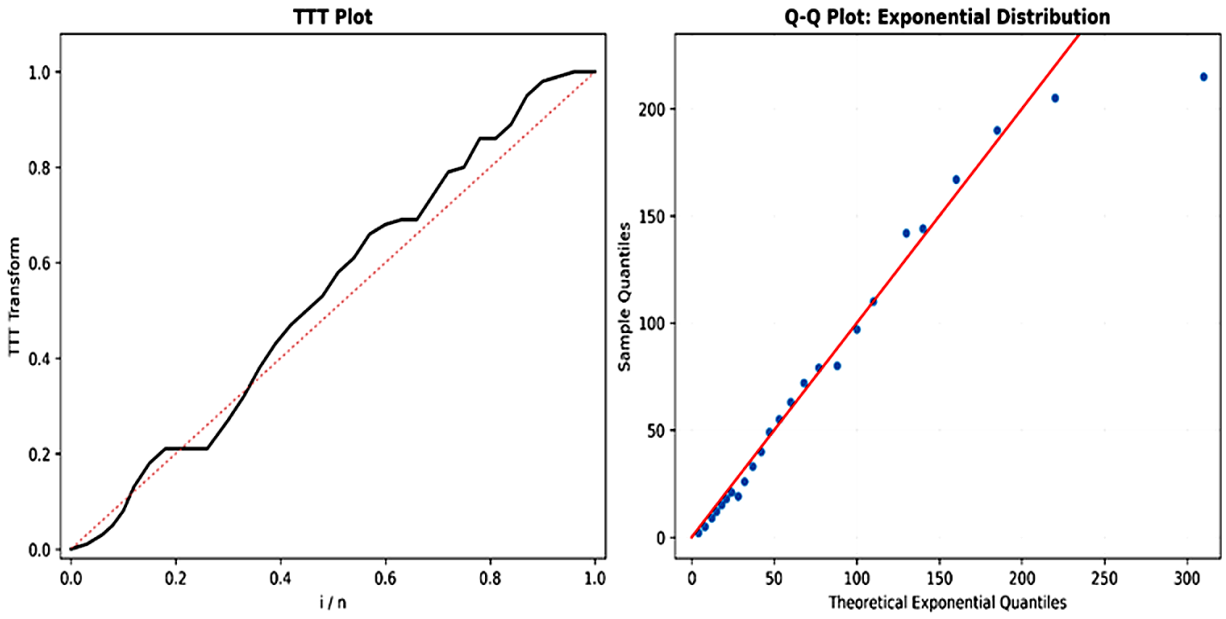

Figure 5. Exponential distribution fitted to Dataset 1.

The computed statistics are

$$\hat{\mathbb{T}}0.6^{*} = 0.2100,\ \hat{\mathbb{T}}0.8^{*} = 0.0978, \text{ and } \hat{\mathbb{T}}_{1.0}^{*} = 0.2206.$$

All associated p-values exceed 0.05, and therefore the null hypothesis of exponentiality is not rejected. This outcome is consistent with a failure mechanism driven primarily by random shocks rather than cumulative wear. The results provide statistical evidence consistent with IFR behavior. However, this conclusion should be interpreted as statistical evidence rather than definitive confirmation of the underlying failure mechanism.

Dataset 2: Flood levels of the susquehanna river

The second dataset, from Seshadri [24], consists of 20 maximum flood levels recorded over four-year intervals. The observations are: 0.654, 0.613, 0.315, 0.449, 0.297, 0.402, 0.379, 0.423, 0.379, 0.3235, 0.269, 0.740, 0.418, 0.412, 0.494, 0.416, 0.338, 0.392, 0.484, and 0.265.

Figure 6 displays the corresponding TTT and Q–Q plots. The TTT curve exhibits a clear concave shape, providing strong graphical evidence of IFR behavior. The computed statistics yield values effectively equal to zero for all three β choices, with p-values substantially below 0.05. The null hypothesis of exponentiality is decisively rejected. This suggests that the underlying stochastic mechanism exhibits increasing risk behavior, possibly reflecting progressive hydrological or environmental effects.

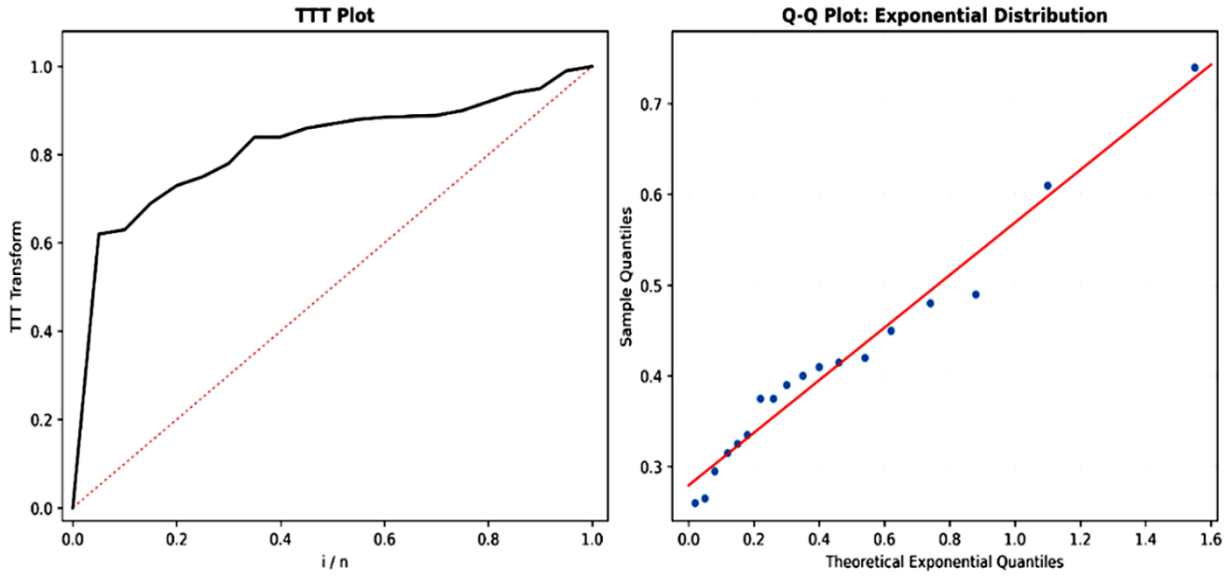

Figure 6. Exponential distribution fitted to Dataset 2.

This finding is strongly confirmed by the proposed test, which yields $\hat{\mathbb{T}}^*_{0.6} = 0.0001$, $\hat{\mathbb{T}}^*_{0.8} = 0.0001$, and $\hat{\mathbb{T}}^*_{1.0} = 0.0001$. The p-values, being substantially less than 0.05, lead to a decisive rejection of the null hypothesis. This statistical evidence suggests that the risk of extreme flood events follows an increasing failure rate pattern, indicating that the likelihood of a severe flood increases over time, possibly due to silting, changes in river morphology, or watershed saturation.

Dataset 3: Mechanical component failures

The third dataset, from Nelson [25], contains 51 failure times of a mechanical snubber component. The observations are: 12, 17, 7, 13, 5,2, 12, 2,6, 4, 5, 14, 6, 2, 4, 18, 4, 19, 5, 14, 20, 8, 11, 26, 1, 3, 10, 18, 6, 10, 23, 7, 20, 4, 7, 6, 12, 10, 20, 3, 12, 3, 18, 18, 14, 14, 8, 6, 22, 11, and 8.

Figure 7 shows a distinctly concave TTT curve, strongly deviating from the diagonal. The Q–Q plot further confirms departure from exponentiality. The proposed test yields statistics near zero for all β values, with p-values well below 0.05, leading to rejection of exponentiality. The results indicate positive aging behavior consistent with mechanical wear and fatigue processes.

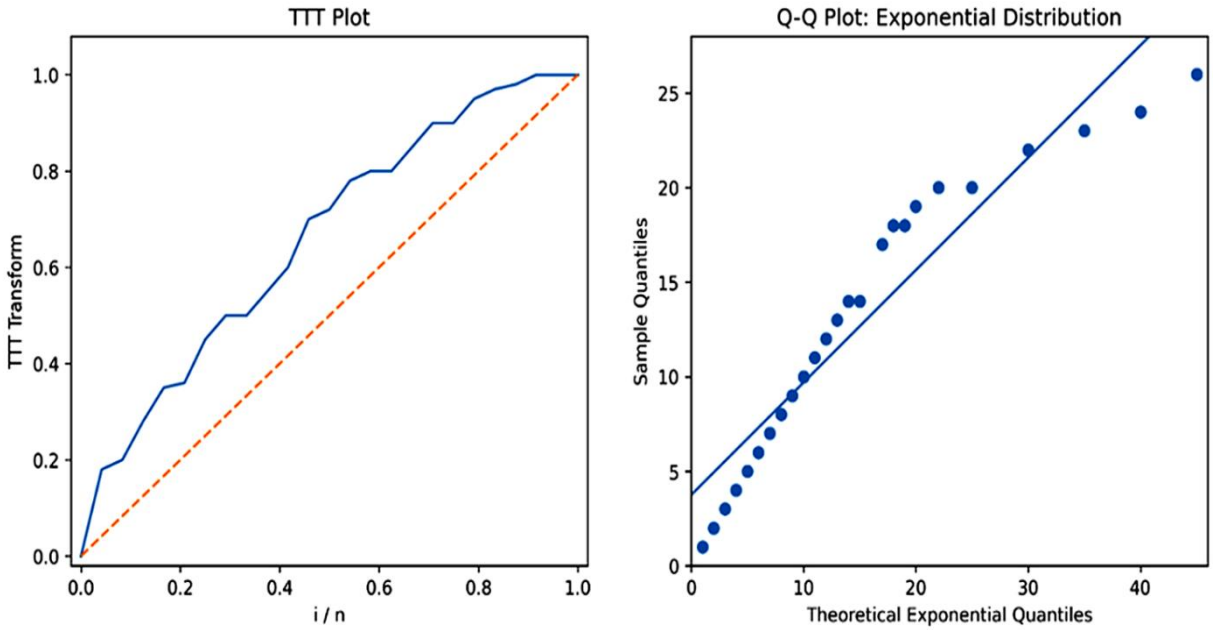

Figure 7. Exponential distribution fitted to Dataset 3.

The graphical analysis in Figure 4 reveals a TTT plot that is distinctly concave, providing strong visual evidence against the constant failure rate assumption. The formal test results are unequivocal, with $\hat{\mathbb{T}}^*_{0.6} = 0.0001, \hat{\mathbb{T}}^*_{0.8} = 0.0001$, and $\hat{\mathbb{T}}^*_{1.0} = 0.0001$. The corresponding pvalues are significantly below 0.05, leading to the rejection of the exponentiality hypothesis. This analysis confirms that the failure mechanism for this mechanical component is characterized by positive aging. The risk of failure increases with operational time, a typical scenario for parts subject to wear, fatigue, and cumulative damage, thereby justifying an IFR model.

Dataset 4: Aquifer thickness measurements

The fourth dataset, analyzed by Thomas and Jose [26], consists of 77 measurements of aquifer thickness. The observations are: 10.49, 8.80, 12.42, 4.58, 6.85, 4.58, 5.00, 4.75, 4.75, 12.25, 9.50, 13.54, 10.42, 4.65, 9.88, 6.21, 8.60, 7.06, 7.96, 7.89, 9.70, 13.90, 12.65, 10.00, 12.65, 12.07, 9.80, 13.54, 9.82, 13.54, 12.42, 12.73, 12.22, 12.25, 12.32, 8.75, 12.00, 17.50, 11.88, 13.13, 13.56, 15.44, 13.22, 7.28, 11.70, 11.70, 11.60, 10.90, 11.84, 8.00, 10.20, 5.77, 13.90, 4.58, 12.07, 15.44, 10.20, 11.00, 8.50, 10.99, 10.39, 9.90, 13.94, 15.21, 13.56, 9.00, 20.47, 15.22, 11.50, 13.90, 13.22, 10.48, 15.48, 9.80, 12.21, 13.56, and 7.04.

Figure 8 presents the TTT and Q–Q plots. The TTT curve again shows a pronounced concave pattern. The formal test confirms this visual evidence, producing very small p-values for all β values and leading to rejection of exponentiality. Although "failure rate" is not directly interpretable in a geological context, the statistical structure of the data exhibits properties analogous to IFR behavior. This suggests systematic departure from a memoryless model and indicates increasing stochastic intensity across the range of observations.

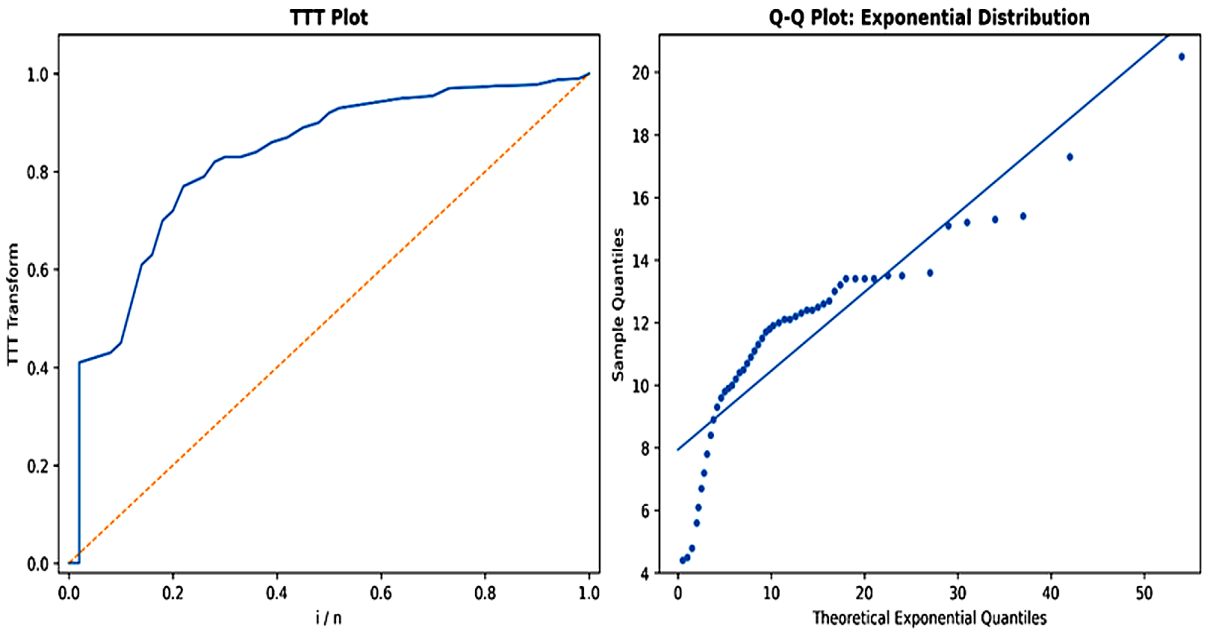

Figure 8. Exponential distribution fitted to Dataset 4.

The formal test confirms this visual cue, with all three test statistics yielding values of $\hat{\mathbb{T}}^*_{0.6} = 0.0001$, $\hat{\mathbb{T}}^*_{0.8} = 0.0001$, and $\hat{\mathbb{T}}^*_{1.0} = 0.0001$. The resulting p-values are far below the 0.05 threshold, leading to the rejection of the exponential distribution. While the concept of a "failure rate" is not directly applicable to a geological formation's thickness, within the framework of this statistical test, the result indicates that the stochastic behavior of the thickness measurements exhibits properties analogous to an IFR distribution. This could imply, for instance, that the probability of encountering a substantially thicker (or more productive) aquifer stratum follows a pattern consistent with positive aging, which may reflect underlying geological deposition or erosion processes. It should be noted that these conclusions are based on statistical testing results and should be interpreted within the limitations of the adopted modeling framework.

5. Conclusions

In this paper, I developed a new entropy-based test family $\hat{\mathbb{T}}^*_{\beta}$ for testing exponentiality against IFR alternatives, one of the central problems in statistical reliability theory. The proposed statistic was constructed from a fractional generalized cumulative residual entropy framework, leading to a scale-invariant L-functional that combines interpretability, computational simplicity, and strong theoretical structure. A principal theoretical contribution of this work is the derivation of the exact finite-sample null distribution under exponentiality. This result enables exact inference without asymptotic approximation and establishes distribution-freeness within the exponential family. In parallel, asymptotic normality was established under general regularity conditions, providing a unified inferential framework that is valid across small and large sample regimes. The Monte Carlo investigation demonstrated that the proposed procedure exhibits strong and stable power across a broad spectrum of IFR alternatives, including LFR, Makeham, and Weibull models. The presence of the

tuning parameter β was shown to meaningfully influences sensitivity, enabling practitioners to adapt the test to anticipated aging structures. Across all considered sample sizes, the statistic maintained competitive and frequently superior performance relative to established competitors, particularly in the moderate-deviation regime where discrimination is most demanding.

The practical applicability of the methodology was further illustrated through four real datasets spanning reliability engineering, hydrology, mechanical systems, and geophysical measurements. In each case, graphical diagnostics via Total Time on Test plots were consistent with the formal testing results, reinforcing the robustness and interpretability of the proposed framework. Beyond its immediate contributions, this work opens several avenues for further investigation. First, an analytical study of optimal or data-driven selection of the tuning parameter β remains an important open problem, potentially involving local asymptotic efficiency or minimax criteria. Second, extension of the proposed entropy-based approach to censored data settings, particularly right-censoring common in survival analysis, would significantly broaden its applicability. Third, the development of analogous tests for other aging classes, such as decreasing failure rate (DFR), bathtub-shaped hazard models, or new better than used (NBU) alternatives, represents a natural generalization. Finally, exploring multivariate or system-level extensions, particularly in dependent reliability structures, offers promising directions for future research.

In summary, the proposed entropy-driven test family provides a theoretically rigorous, flexible, and practically effective methodology for detecting departures from exponentiality toward positive aging. By integrating information-theoretic functionals with a classical L-statistic structure and exact distribution theory, this work contributes a robust and adaptable tool to modern reliability and lifetime data analysis.

Use of Generative-AI tools declaration

The author declares he has not used Artificial Intelligence (AI) tools in the creation of this article.

Funding

The author acknowledges financial support from the Deanship of Graduate Studies and Scientific Research at Qassim University (Grant No. QU-APC-2026).

Conflicts of interest

The author declares no conflict of interest.

References

1. F. Proschan, R. Pyke, Tests for monotone failure rate, In: *Fifth Berkeley Symposium on Mathematical Statistics and Probability*, 1967, 293–312.
2. P. J. Bickel, K. A. Doksum, Tests for monotone failure rate based on normalized spacings, *Ann. Math. Statist.*, **40** (1969), 1216–1235. https://doi.org/10.1214/aoms/1177697498
3. P. J. Bickel, Tests for monotone failure rate II, *Ann. Math. Statist.*, **40** (1969), 1250–1260. https://doi.org/10.1214/aoms/1177697500

4. R. E. Barlow, F. Proschan, A note on tests for monotone failure rate based on incomplete data, *Ann. Math. Statist.*, **40** (1969), 595–600. https://doi.org/10.1214/aoms/1177697727
5. R. E. Barlow, K. A. Doksum, Isotonic tests for convex orderings, In: *Proceedings of the Sixth Berkeley Symposium on Mathematical Statistics and Probability*, **1** (1972), 293–323.
6. I. A. Ahmad, A nonparametric test for the monotonicity of a failure rate function, *Commun. Statist.*, **4** (1975), 967–974. https://doi.org/10.1080/03610927508827305
7. J. V. Deshpande, S. C. Kochar, A test for exponentiality against IFR alternatives, *IAPQR Trans.*, **8** (1983), 1–8.
8. B. Klefsjö, Some tests against aging based on the total time on test transform, *Commun. Stat. Theor. M.*, **12** (1983), 907–927. https://doi.org/10.1080/03610928308828505
9. A. A. Aly Jumad-Eldust, On some tests for exponentiality against IFR alternatives, *Statistics*, **21** (1990), 217–226. https://doi.org/10.1080/02331889008802242
10. M. Mitra, M. Z. Anis, An L-statistic approach to a test of exponentiality against IFR alternatives, *J. Stat. Plan. Infer.*, **138** (2008), 3144–3148. https://doi.org/10.1016/j.jspi.2007.12.005
11. M. Z. Anis, A family of tests for exponentiality against IFR alternatives, *J. Stat. Plan. Infer.*, **143** (2013), 1409–1415. https://doi.org/10.1016/j.jspi.2013.03.012
12. A. Di Crescenzo, S. Kayal, A. Meoli, Fractional generalized cumulative entropy and its dynamic version, *Commun. Nonlinear Sci.*, **102** (2021), 105899. https://doi.org/10.1016/j.cnsns.2021.105899
13. A. A. Alqefari, G. Alomani, F. Alrewely, M. Kayid, Information-theoretic reliability analysis of consecutive r-out-of-n: G systems via residual extropy, *Entropy*, **27** (2025), 1090. https://doi.org/10.3390/e27111090
14. G. Alomani, M. Kayid, Stochastic properties of fractional generalized cumulative residual entropy and its extensions, *Entropy*, **24** (2022), 1041. https://doi.org/10.3390/e24081041
15. M. Asadi, N. Ebrahimi, E. S. Soofi, Connections of Gini, Fisher and Shannon by Bayes risk under proportional hazards, *J. Appl. Probab.*, **54** (2017), 1027–1050. https://doi.org/10.1017/jpr.2017.51
16. M. Kayid, M. Shrahili, Information properties of consecutive systems using fractional generalized cumulative residual entropy, *Fractal Fract.*, **8** (2024), 568. https://doi.org/10.3390/fractalfract8100568
17. G. E. P. Box, Some theorems on quadratic forms applied in the study of analysis of variance problems I, *Ann. Math. Statist.*, **25** (1954), 290–302. https://doi.org/10.1214/aoms/1177728786
18. S. M. Stigler, Linear functions of order statistics with smooth weight functions, *Ann. Statist.*, **2** (1974), 676–693. https://doi.org/10.1214/aos/1176342756
19. B. L. Jones, R. Zitikis, Empirical estimation of risk measures and related quantities, *N. Am. Actuar. J.*, **7** (2003), 44–54. https://doi.org/10.1080/10920277.2003.10596117
20. I. A. Ahmad, I. A. Al-Wasel, A. H. El-Bassiouny, M. Kayid, A new approach to moments inequalities of some aging notions with hypotheses testing applications, *J. Appl. Probab. Stat.*, **2** (2007), 71–88.
21. I. A. Ahmad, Moments inequalities of aging families of distributions with hypotheses testing applications, *J. Stat. Plan. Infer.*, **92** (2001), 121–132. https://doi.org/10.1016/S0378-3758(00)00139-7
22. R. E. Barlow, R. Campo, Total time on test processes and applications to failure data analysis, In: *Reliability and fault tree analysis*, 1975.

23. F. Proschan, Theoretical explanation of observed decreasing failure rate, *Technometrics*, **5** (1963), 375–383. https://doi.org/10.2307/1266340
24. V. Seshadri, *The inverse Gaussian distribution: Statistical theory and applications*, New York: Springer, 2012. https://doi.org/10.1007/978-1-4612-1456-4
25. W. Nelson, *Applied life data analysis*, New York: Wiley, 1982. https://doi.org/10.1002/0471725234
26. P. Y. Thomas, J. Jose, On Weibull-Burr impounded bivariate distribution, *Jpn. J. Stat. Data Sci.*, **4** (2021), 73–105. https://doi.org/10.1007/s42081-020-00085-w

AIMS Press